

# New conception of 3×4 circularly polarized antenna patch network for radio frequency energy harvesting at 2.45 GHz

Walid En-Naghma, Hanan Halaq, Abdelghani El Ougli

Department of Physics, Computer Science, Signal, Automation, and Cognitivism Laboratory, Faculty of Sciences, Sidi Mohamed Ben Abdellah University, Fez, Morocco

## Article Info

### Article history:

Received Mar 30, 2023

Revised Jun 12, 2023

Accepted Jun 17, 2023

### Keywords:

Circular polarization

Micro-ribbon line

Microstrip antenna

Planar antenna array

Triangular form shaped

Wireless power transmission

## ABSTRACT

This paper presents a developed design of a 3×4 circular polarization microstrip antenna patch array whose resonance frequency is 2.45 GHz in the industrial, scientific, and medical (ISM) band. This array is printed on a FR4 substrate of 1.58 mm thickness with a dielectric permittivity of 4.4. The basic antenna patch is a square shape inserted by a rectangular slot inclined positioned diagonally at the center to achieve circular polarization. In addition, a triangular-shaped slit is added at each of the four corners of the patch. The antenna array performance is tested numerically using two different software packages, CST MWS and HFSS. The antenna's array size is compacted to a 22.7×13.5 cm. The simulated results give good performance results in terms of return loss and gain; directivity is found to be 9.66 dBi at 2.45 GHz; the axial ratio value is 1.69 dB; and total efficiency is about 95.55% at 2.45 GHz. Then, the simulated results obtained by these two programs are in good agreement, which makes this proposed array design very suitable for radio frequency energy harvesting and its various applications to power supply different devices in a clean way for our environment.

*This is an open access article under the [CC BY-SA](https://creativecommons.org/licenses/by-sa/4.0/) license.*



## Corresponding Author:

Walid En-Naghma

Department of Physics, Computer Science, Signal, Automation, and Cognitivism Laboratory

Faculty of Sciences, Sidi Mohamed Ben Abdellah University

B.P.1796 Fez-Atlas, 30003, Fez, Morocco

Email: walid.ennaghma@usmba.ac.ma

## 1. INTRODUCTION

Wireless devices such as smartphones, tablets, drones, and sensor networks are very useful in all areas, which leads to an increasing use of batteries. Unfortunately, the batteries have expired due to their limited life cycle, their very expensive and difficult recycling, their large occupied surfaces, and their complex positions in places inaccessible, especially for sensor networks. To avoid all these problems mentioned above, a promising solution is available that is based on capturing electromagnetic waves and storing them afterwards. This solution is included in the technology known as wireless power transmission (WPT), which is more prevalent and more recent in research [1]–[4].

Solar space energy transmission (SPT) and wireless microwave energy transmission WPT have become interesting topics in the last few centuries for transmitting energy in the future. The WPT has been known since the early 1900s, when Nikola Tesla who theorized, developed, demonstrated, and used this concept in many real-world applications. The high motivation in WPT over the last few decades is due to these many advantages: the transmission of electrical energy to loads without wired connections, that ensures the autonomy of the mains socket [5], the elimination and reduction of interconnected cables and wires in order to avoid short circuits, and the reduction of the wireless devices weight by eliminating batteries that have a significant weight.

In recent years, researchers have become increasingly interested in microwave power transmission (MPT) systems such as rectenna systems [6], [7]. The rectenna systems consist of two parts: the emitting part and the receiving part. The main purpose of rectenna systems is to convert the DC power supply into micro-radiation waves by means of a transmitter antenna. After, to transmit this radiation in the free space to a receiver antenna which in turn receives this micro-radiation waves and convert it into useful DC power. Rectenna systems consist of an antenna integrated with a rectification circuit. The first appearance of the rectenna system was by W. Brown in the United States, whose revolutionary work he did at MPT in 1960 at Raytheon Technology Company in the United States. In addition, W.C. Brown showed the great ability of MPT to launch a microwave helicopter alone, as in [8]. This MPT revolution in [9]–[11] has crushed all fields. In the literature, the rectenna systems studied operate on several operating frequencies from 2.45 GHz to 5.8 GHz, as in [12]–[14], because these two operating frequencies of 2.45 GHz and 5.8 GHz have a relatively low atmospheric loss.

The blocks of the rectenna's basic architecture are illustrated in Figure 1 as in [15], [16]. This figure is added to explain the main functions of the rectenna system. The first block concerns the receiving antenna, which collects microwave energy and converts it into DC using a rectifying circuit. The second block is the high-frequency filter (HF filter) added between the receiving antenna and the rectification circuit to prevent the antenna from re-irradiating the higher-order harmonics generated by the rectification circuit. The third block is the rectification circuit. The fourth block is a direct current filter (DC filter) added between the rectification circuit and the load represented by the last block to prevent the loading of radio frequency signals. The load is the rectenna's final component. It is represented by the input impedance of one or more devices that will be connected to the desired application.

The rectenna system has been studied for different types of polarization, such as linear polarization (LP) as in [17]–[20], and circular polarization (CP) as in [21]–[24]. In this paper, the main contribution is CP because the CP leads to an almost constant DC output when the receiving antenna or transmitting antenna changes direction in space. The main contribution in this article is to propose a new design of a circular polarized antenna patch array that operates at the 2.45 GHz resonance frequency in the industrial, scientific, and medical (ISM) band, which is characterized by excellent performance in terms of return loss, gain, directivity, axial ratio, and total efficiency. This developed array design will be used in the rectenna systems in order to harvest a large amount of incoming power at 2.45 GHz in the ISM band. The developed basic antenna is used to design an antenna array of six identical elements. Each element is a square antenna with rectangular slot inclined in the center and a triangle-shaped slits at the four corners. The elements are connected to a T-Junction power divider to match the antenna input impedance to 50  $\Omega$ .

The construction of this paper has four parts. The first part is the introduction, which gives a brief overview of the antenna patches and their utilities in the rectenna systems for RF energy harvesting. The second part lists the method that explains the structure of the antenna and the steps of the antenna patch design, and in this part where a new design for the antenna patch has been developed. The third part presents the numerical simulation results, discusses them, and compares them to existing work in the literature. This ensures that the proposed novel design has good performance. Finally, the last part devotes itself to the conclusion, which summarizes the main points of this article.

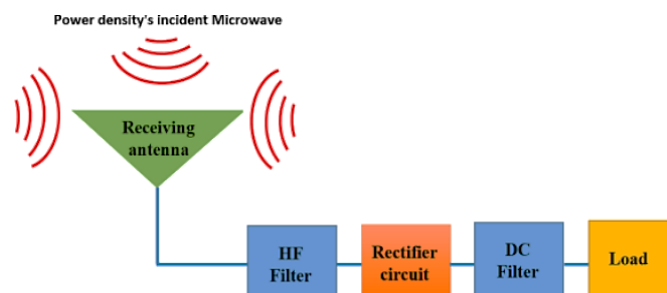


Figure 1. Blocks of the basic rectenna architecture

## 2. METHOD

### 2.1. Antenna structure

The antenna is a converter of electrical energy to electromagnetic energy in the case of a transmitting antenna, or vice versa in the case of a receiving antenna. The most widely used antenna technology in frequency energy (RF) energy harvesting is a patch antenna technology. This technology has several advantages, among which are the following:

- Its wide variety of geometric shapes makes them applicable to different integration situations;
- Its ease of integration thanks to advances in microelectronics technology in the fields of miniaturization and electronic integration;
- Its low weight;
- Its reduced volume;
- Compliance on planar and non-planar surfaces;
- Its ease of manufacture;
- Its various useful polarizations, such as LP and CP;
- Its flexibility in terms of operating frequency.

The general structure of a patch antenna contains of three important elements: the ground plane, the substrate, and the last one, the patch. Figure 2 shows the basic structure of the patch antenna, and Figure 3 illustartes the various geometric forms of the patch as in [25]–[27]. The ground plane, also called ground, is conductive in nature and characterized by the conductivity of the conductor chosen, such as copper, silver, and gold. The substrate, also called the dielectric substrate, is placed on the ground plane. This substrate is defined by a dielectric constant and an electric dissipation factor (tangential loss).

The patch, also called the radiating element, is placed on the substrate. The patch can take various geometric shapes see Figure 3 that affect the nature of the radiation and also the modes that are likely to excite the antenna. Power to the patch antenna is supplied by feeding the radiating element. There are several power supply methods for feeding the patch such as the micro-ribbon line method, the coaxial probe method, the method of power supply by micoruban line and slit, and the coupled line feed method see the online version of Figure 4.

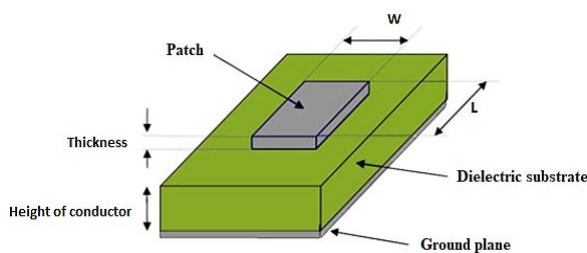


Figure 2. Basic structure of patch antenna

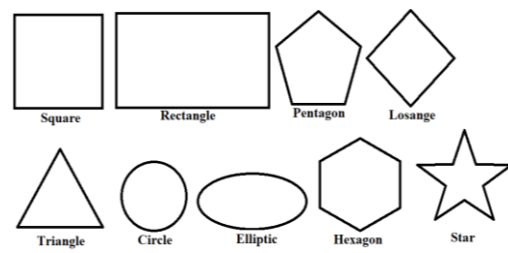


Figure 3. Various geometric shapes of the patch

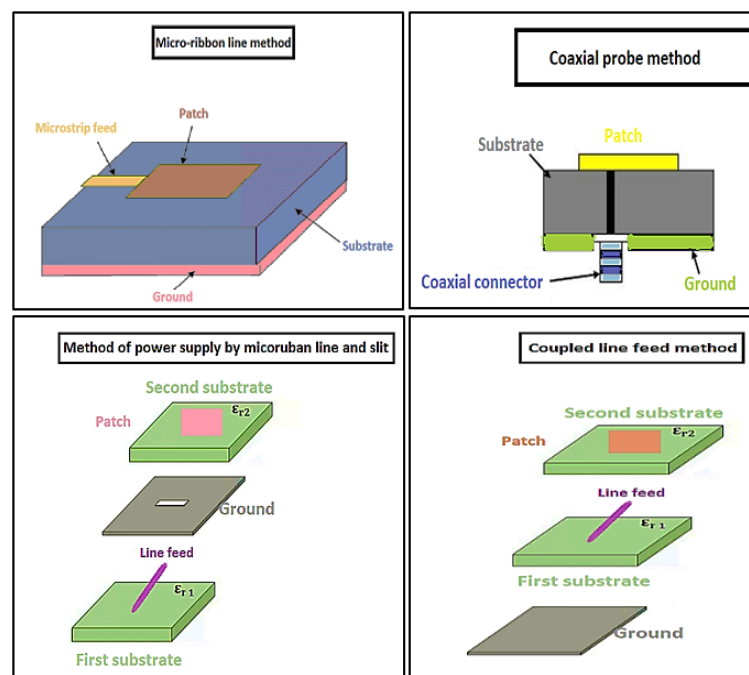


Figure 4. Various power methods for feeding the patch

The main antenna characteristics used to define the performance of the antenna patch are: the coefficient of reflection (i.e., the return loss), voltage standing wave ratio (VSWR), gain, directivity, and bandwidth. In the case of a high-performance antenna, one says that this antenna is able to use it in wireless power transmission applications to power various devices in several areas such as industrial, medical, aerospace, scientific, public, power supply sensors, drones, smartphones, and brain-machine interface. Throughout this paper, we will focus on the patch antenna with a square shape of the radiating element with circular polarisation at a resonant frequency of 2.45 GHz in the ISM band and powered by the microstrip line through a single excitation port.

## 2.2. Patch antenna design

### 2.2.1. Design phase

The process of designing a patch antenna, also known as the patch antenna design phase, namely; i) specify the value of the operation frequency, that is, the value of the resonance frequency noted  $f_r$ ; ii) specify the substrate permittivity value (i.e., the substrate dielectric constant) noted  $\epsilon_r$ ; iii) specify the height of the substrate (i.e., the substrate thickness) noted  $h_s$ ; and iv) using the specified parameters ( $f_r$ ,  $\epsilon_r$  and  $h_s$ ), determine the patch's width  $W_p$  and the patch's length  $L_p$  using the equations that will be mentioned in the next subsection (2.2.2.). Figure 5 is intended to illustrate the design phase.

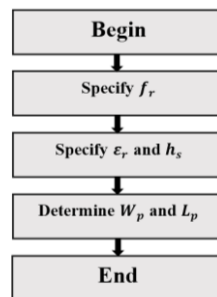


Figure 5. Patch antenna design flowchart

### 2.2.2. Theoretical design

Equations can be found in the literature to facilitate the calculation of the radiating element dimensions, as in [28]. In (1) is used to calculate the patch's width ( $W_p$ ). In (2) is used to calculate the dielectric effective permittivity ( $\epsilon_{reff}$ ). The patch's length ( $L_p$ ) is extended by a distance ( $\Delta L_p$ ) due to fringe phenomena, where in (3) is used to calculate  $\Delta L_p$ . The wavelength ( $\lambda$ ) depends on the resonance frequency ( $f_r$ ) and the speed of light in a vacuum ( $C$ ), where in (4) is used to calculate the wavelength. In (5) is employed to calculate the patch's length ( $L_p$ ).

$$W_p = \frac{C}{2f_r} \sqrt{\frac{2}{\epsilon_r + 1}} \quad (1)$$

$$\epsilon_{reff} = \frac{\epsilon_r + 1}{2} + \frac{\epsilon_r - 1}{2} \left[ 1 + 12 \frac{h_s}{W_p} \right]^{-1/2} \quad (2)$$

$$\Delta L_p = 0.412 h_s \left( \frac{\epsilon_{reff} + 0.3}{\epsilon_{reff} - 0.258} \right) \left( \frac{W_p/h_s + 0.264}{W_p/h_s + 0.8} \right) \quad (3)$$

$$\lambda = \frac{C}{f_r} \quad (4)$$

$$L_p = \frac{\lambda}{2} - \Delta L_p \quad (5)$$

### 2.2.3. Analysis phase

The analysis phase is used for a parametric study to optimize the dimensions of the patch antenna to be designed according to the required specifications. In other words, the analysis phase is the simulation phase

where these optimized dimensions are obtained using the full-wave simulator called computer simulation technology (CST) on a personal computer (PC) with Windows 10 professional, an Intel (R) Core (TM) i5 5300U CPU, 2.30 GHz, and 8.00 GB of RAM. Figure 6 depicts a flowchart of the patch antenna analysis method, which illustrates the steps involved in designing a patch antenna step by step.

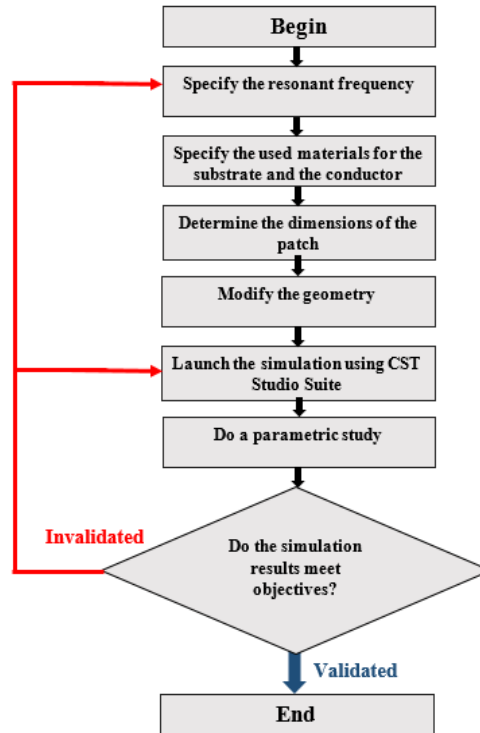


Figure 6. Patch antenna analysis method flowchart

**2.3. New patch antenna design**

In this article, a novel design of circularly polarized patch antenna operating at a resonant frequency of 2.45 GHz has been developed. With the radiating element designed with a modified square geometry. The proposed design is fed by a microstrip line through a single excitation port.

**2.3.1. Substrate selection**

The choice of substrate has a very important task in the design of the patch antenna, as it affects its performance. The correct choice of substrate is used to meet the design specifications. Therefore, in order to make a precise choice of the type of substrate, it is necessary to choose as well as possible the parameters that define this substrate, which are the dielectric constant  $\epsilon_r$  and the tangential loss  $\tan(\delta)$ . The type of substrate used in our new patch antenna design is the FR4-expoy material. The characteristics of the substrate suitable for this developed design are:

- The relative permittivity  $\epsilon_r$ , equal to 4.4;
- The thickness  $h_s$ , equal to 1.58 mm;
- The tangential loss  $\tan(\delta)$ , equal to 0.001.

**2.3.2. Basic antenna design developed**

The developed design of the basic antenna is described by its square-shaped radiating element with a modification at its four corners in the form of a triangular truncation and by the insertion of an oblique rectangular slot in the center of the square patch fed by a single excitation port at 50 ohms. The proposed design is an improved design using two techniques:

- The truncation technique allows the bandwidth around the operating frequency to be increased and the total patch area to be minimized [29];
- The slit technique, which improves the performance of the patch antenna in terms of axial ratio and reflection coefficient [29].

The dimensions of this basic antenna are obtained using the equations mentioned above. Figure 7 shows the improved design of the basic antenna patch by showing the values of its dimensions after an optimization process of these different dimensions to find the optimal dimensions for this antenna to function properly. This improvement has been achieved thanks to the performance provided by truncation and slotting techniques.

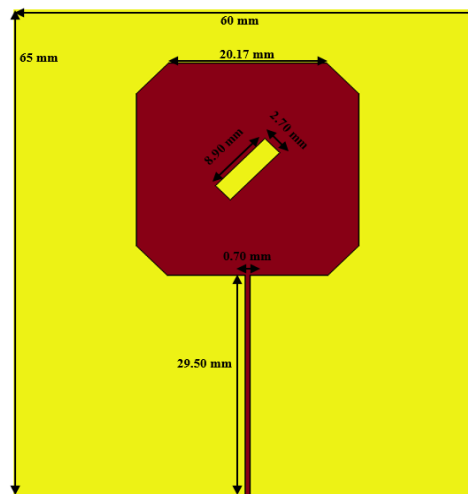


Figure 7. Basic antenna patch structure and its dimensions

### 2.3.3. Antenna array design developed

The array antenna patch is based on the basic antenna patch design proposed in this paper. The new design developed for this array is intended to improve its performance of this array. This array antenna achieves directivity and significant gain due to the number of basic radiators used in the network and the increase in the collection area. The developed network antenna design contains six basic antenna elements, so one can say that this network is considered a  $3 \times 4$  network (i.e., 3 rows and 4 columns). This design makes use of the advantages of the two techniques mentioned above, namely the tilted slit technique and the triangular truncation technique, at the four corners of the radiating element. Thus, this design respects the same distance between the basic antennas by exciting them in a uniform way, that is, each of its basic antennas has an equal excitation to that of its neighboring basic antenna. Figure 8 depicts the design of the proposed array antenna, giving the dimensional values after an optimization process for these different dimensions. The optimization process makes it possible to find the optimum dimensions of this array antenna to work well with better performance.

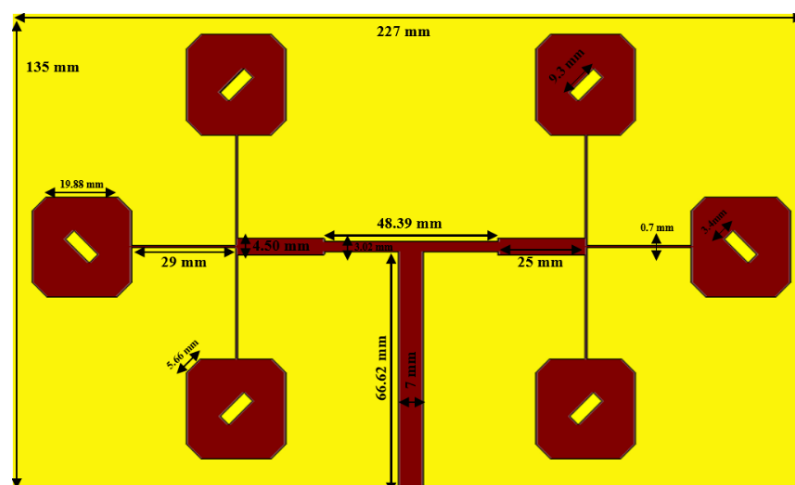


Figure 8. Antenna patch array structure and its dimensions

### 3. RESULTS AND DISCUSSION

The simulated results of key parameters help us to discuss the performance of the basic antenna patch and the network antenna patch developed in this work. The CST MWS software was the primary tool used to simulate results, but some results were also obtained using the HFSS solver. The variation of the return loss according to frequency is illustrated in Figure 9. At the 2.45 GHz resonance frequency, the reflection coefficient is equal to -27.79 [dB] using CST software and it equal to -13.63 [dB] using the HFSS solver; this value is less than -10 [dB]. The basic antenna operates with adequate adaptation in a band from 2.431 GHz to 2.478 GHz using CST software, i.e., the bandwidth is equal to 47 MHz. The results obtained by the two software programs CST MWS and HFSS show that this basic antenna works well at 2.45 GHz with an adequate adaptation to the excitation port of 50 ohms.

The VSWR variation according to frequency is shown in Figure 10. At the 2.45 GHz operating frequency, the VSWR is equal to 1.08 using CST software and equal to 1.52 using an HFSS solver; this value is close to 1. The basic antenna patch operates with adequate adaptation at 2.45 GHz. The results obtained by the two solvers CST and HFSS show that this basic antenna operates well at 2.45 GHz with adequate adaptation to the excitation port of 50 Ω. The basic antenna’s two-dimensional polar view directivity of the radiation pattern at 2.45 GHz in the ISM band is illustrated in Figure 11. The main lobe magnitude of 6.33 [dBi], the main lobe direction of 7 degrees, and the angular width (3 dB) of 91.5 degrees.

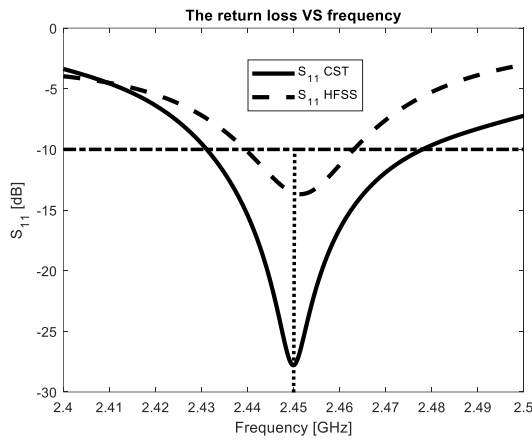


Figure 9. Return loss vs frequency

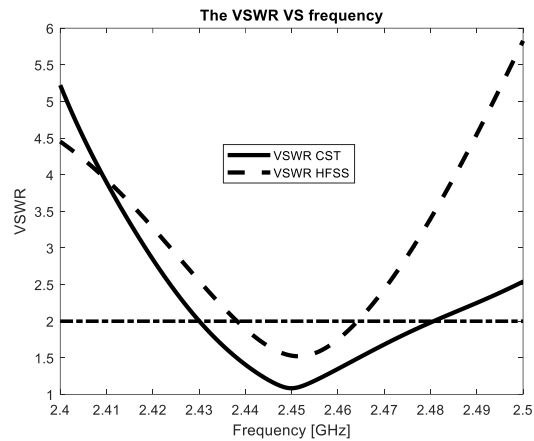


Figure 10. VSWR vs frequency

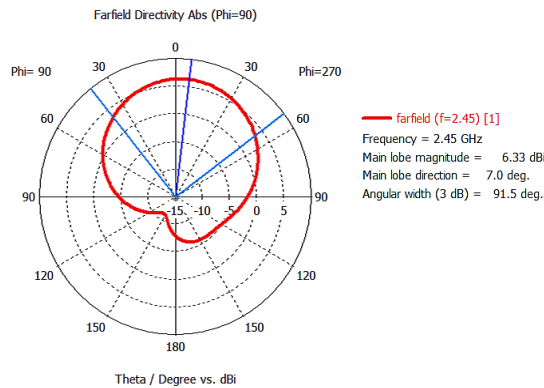


Figure 11. 2D polar radiation pattern

A study was conducted to understand and illustrate the influence of the rectangular slot dimensions, width in Figure 12 and length in Figure 13 on the performance of the array antenna patch, such as the reflection coefficient. The results of the return loss simulations extracted by the CST MWS software show that when the width of the slot is reduced by fixing its length, the resonance frequency is offset to the high frequencies. However, when the width of the slot is increased by fixing its length, the resonance frequency is offset to the low frequencies. The optimum value of this width is obtained at 3.4 mm. The simulated results of the return

losses obtained by CST show that when we increase the length of the slot by fixing its width, it leads to an offset of the resonant frequency towards the low frequencies. However, when we decrease the length of the slot by fixing its width leads to an offset of the resonant frequency towards the high frequencies. The optimum value of this length is 9.3 mm. Therefore, these optimal values of the length and width of the rectangular slot have a good impedance adaptation level of  $-42.65$  [dB].

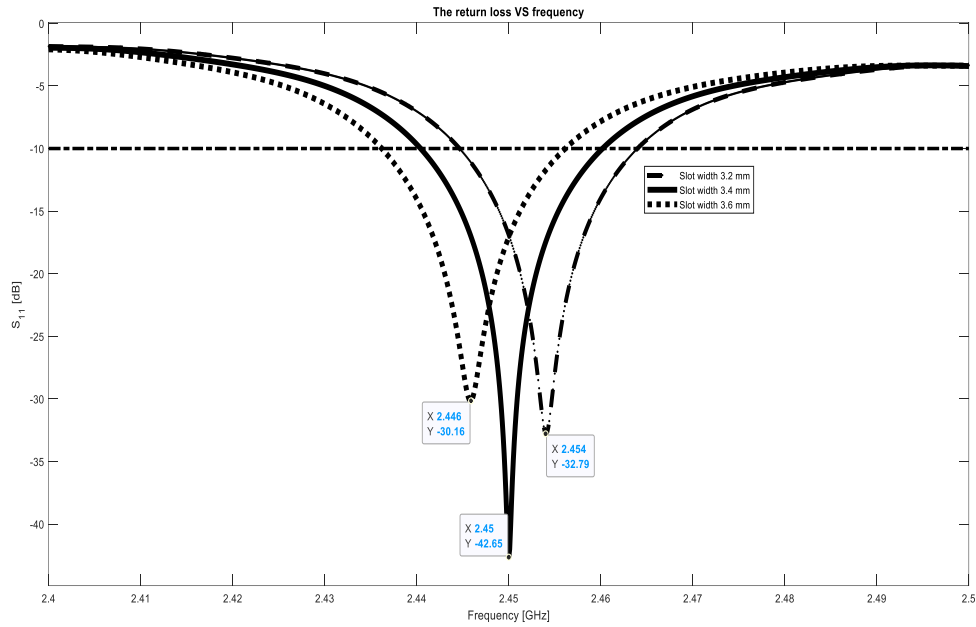


Figure 12. Return loss versus frequency for different widths

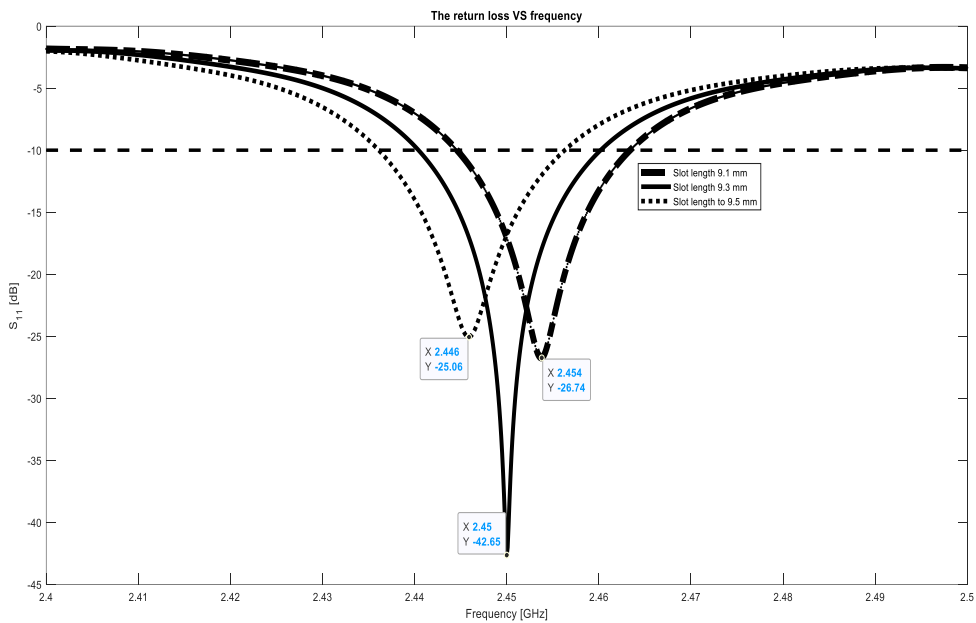


Figure 13. Return loss versus frequency for different lengths

Figure 14 shows the curve of the reflection coefficient as a function of the frequency of the array antenna. The network antenna reflection coefficient value is equal to  $-42.65$  [dB] at 2.45 GHz using CST software, and it is equal to  $-22.96$  [dB] at 2.45 GHz using the HFSS solver. The differences in the results obtained by CST and HFSS can be attributed to the different numerical methods used by the two simulators.

The array antenna patch operates with adequate adaptation in a band from 2.44 GHz to 2.46 GHz using CST software, i.e., the bandwidth is equal to 20 MHz. Return loss is a crucial parameter for an antenna as it reveals the amount of energy lost and provides insights into the energy transfer efficiency and impedance matching. In the case of this array antenna patch, it exhibits excellent impedance adaptation, low losses, and maximum energy transfer, indicating its superior performance. The voltage standing wave ratio as a function of the frequency is depicted in Figure 15. At the 2.45 GHz resonance frequency, the VSWR is equal to 1.01 using CST software and equal to 1.15 using an HFSS solver; this value is close to 1. The network antenna patch operates with adequate adaptation at 2.45 GHz. The results obtained by the two solvers CST and HFSS show that this network antenna operates well at 2.45 GHz with an adequate adaptation to the excitation port of value 50 Ω. Therefore, this array antenna is well adapted and delivers maximum power with low losses.

The variation of the input impedance according to the frequency of the proposed design of an array antenna is illustrated in Figure 16. The value of the real part of the array antenna input impedance, also called the resistance, is equal to 27.58 Ω at the operating frequency of 2.45 GHz. The value of the imaginary part of the network antenna input impedance, also called the reactance, is equal to 0 Ω at the operating frequency of 2.45 GHz. So, the input impedance of the array antenna is equal to 27.58+0j at the operating frequency of 2.45 GHz so this array is well suited to the excitation port of value 50 Ω.

The axial ratio as a function of frequency is shown in Figure 17. The axial ratio value is equal to 1.698 [dB] at the 2.45 GHz resonance frequency. This value is less than 3 [dB] which shows that this array works with circular polarization.

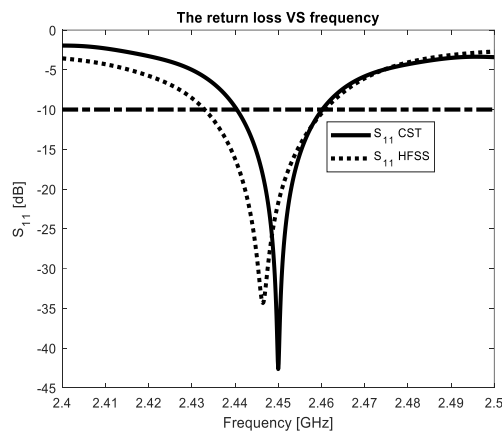


Figure 14. Return loss vs frequency

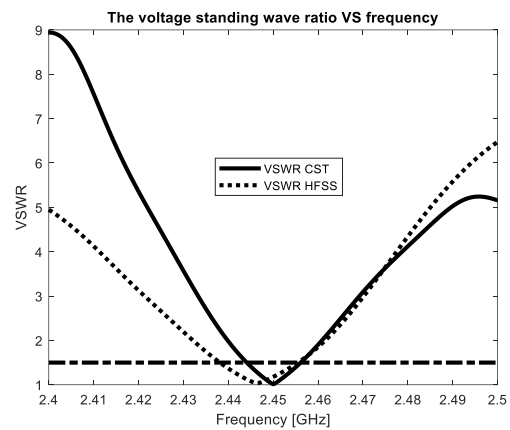


Figure 15. VSWR vs frequency

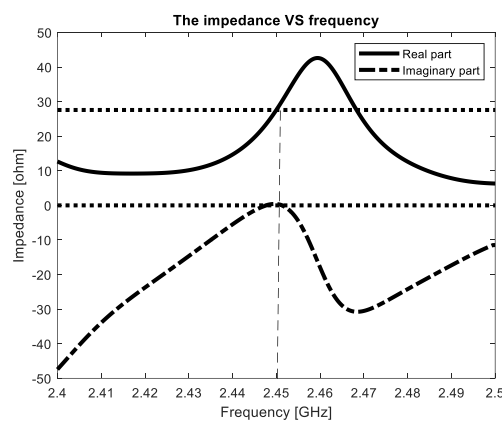


Figure 16. Input impedance vs frequency

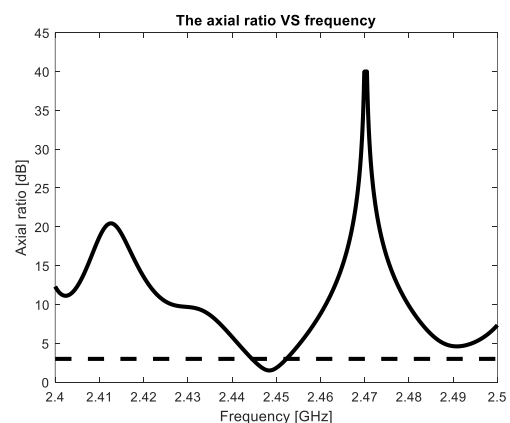


Figure 17. Axial ratio vs frequency

The three simulated powers at the input of the port according to the frequency obtained by the CST software of the 3×4 antenna array are depicted in Figure 18: the first one is the power accepted, the second one is the power reflected, and the last one is the power radiated. The power accepted is 0.4999 W at 2.45 GHz,

the power radiated is equal to 0.4777 W at 2.45 GHz, and the power reflected is  $2.7184 \times 10^{-5}$  W at 2.45 GHz. These results extracted at the resonance frequency of 2.45 GHz for these three powers show that this antenna array has a good level of adaptation at the level of return loss and input impedance at 2.45 GHz. Moreover, this antenna array transfers the maximum amount of energy with the minimum quantity of losses in metal and dielectric.

The radiation efficiency as a function of frequency is shown in Figure 19. The maximum radiation efficiency is 95.56% at 2.45 GHz. This shows that the proposed design of this network has good performance and works well at 2.45 GHz in the ISM band. The gain of this  $3 \times 4$  network is 9.467 [dBi] at 2.45 GHz, and the directivity of this network is 9.655 [dBi] at 2.45 GHz. The gain and directivity results simulated by the CST software as a function of frequency are shown in Figure 20. This figure proves that the network proposed in this paper is effective in terms of gain and directivity at the operating frequency of 2.45 GHz. The total efficiency curve as a function of frequency is shown in Figure 21. At the resonance frequency of 2.45 GHz, the total efficiency value is equal to 95.55%. This total efficiency value ensures that the proposed array in this work operates well at the operating frequency of 2.45 GHz.

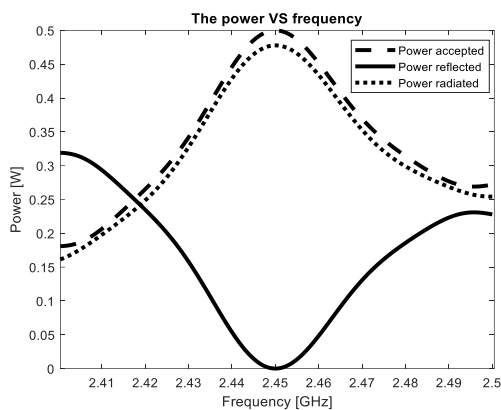


Figure 18. Powers vs frequency

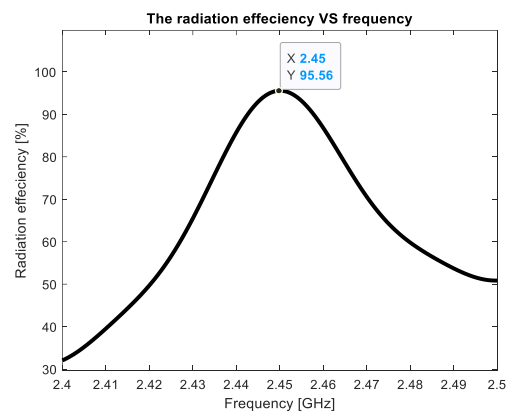


Figure 19. Radiation efficiency vs frequency

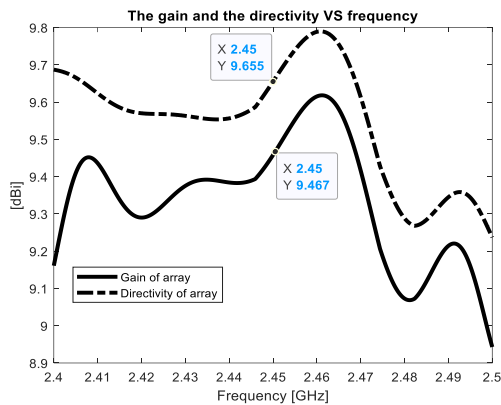


Figure 20. Gain and directivity vs frequency

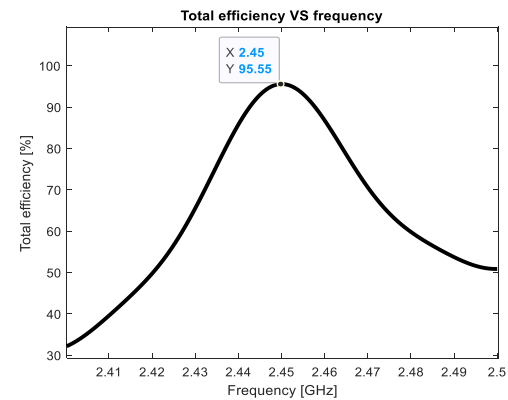


Figure 21. Efficiency vs frequency

The two-dimensional polar view directivity of the radiation pattern for the  $3 \times 4$  antenna patch array at 2.45 GHz is depicted in Figure 22. The main lobe magnitude of 9.69 [dBi], the main lobe direction of 32 degrees, and the angular width (3 dB) is equal to 40.5 degrees. Figure 23 shows the 3D radiation pattern at 2.45 GHz of this array.

Figure 24 shows the manner in which the surface current distribution flows on the six patches of the  $3 \times 4$  antenna patch array. From this result, one can observe that the circulation of the current has a uniformly high strength. Moreover, the current radiates uniformly along the transmission line and the boundary of the six patches of this array uniformly. Also, the boundary of the slits and the inclined rectangular slot supported an important radiating area see the online version of Figure 24. Table 1 summarizes some of the results of antenna

patch networks operating at a 2.45 GHz resonance frequency in the literature. This table helps us make a comparison between the conception developed in this article and other results of literature.

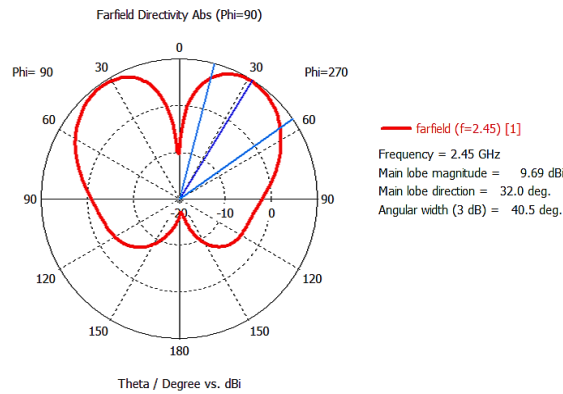


Figure 22. 2D polar radiation pattern

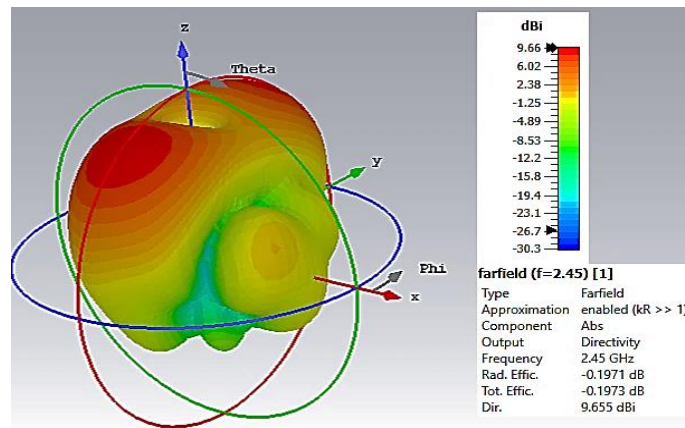


Figure 23. 3D radiation pattern

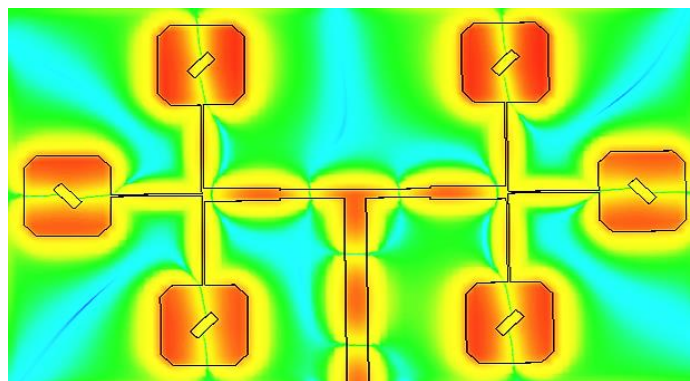


Figure 24. Surface current distribution at 2.45 GHz

Table 1. Comparison of CST software results

Reference	Antenna patch type	Directivity [dBi]
Zbitou <i>et al.</i> [17]	LP 4 elements patches array	7 [dBi]
Sennouni <i>et al.</i> [15]	CP 6 elements patches array	9.14 [dBi]
Sennouni <i>et al.</i> [29]	CP 6 elements patches array	9.153 [dBi]
Figure 8 (our developed design)	CP 6 elements patches array	9.655 [dBi]

From this table, we note that the developed design of the 3×4 network is more efficient in terms of directivity than the other cited works. So, we conclude that this developed network in this paper is better in terms of directivity, and works well at 2.45 GHz with a CP, and is well adapted in terms of the return loss. Our 3×4 array design will be used in all applications that rely on WPT in a variety of areas, such as aerospace applications, wireless sensor networks, automotive applications for charging electric vehicle batteries, brain-machine interface systems in medicine, neural registration systems in medical fields, and wireless mobile chargers.

#### 4. CONCLUSION

In this paper, a novel design of 3×4 circular polarization microstrip antenna patch array operating at the resonance frequency of 2.45 GHz in the ISM band is mounted on a FR4 substrate. The basic antenna patch is a square-shaped metal sheet with an angled rectangular slot in the center and inserted by a triangular-shaped slit at the four corners. An excellent agreement is found between the antenna performance results extracted by two various software programs, CST MWS and HFSS. The good performance of this developed design in terms of return loss of -42.65 dB, axial ratio of 1.69 dB, directivity of 9.66 dBi, gain of 9.47 dBi, and total efficiency of 95.55%. These simulated results make this design very suitable for RF energy harvesting and their different applications to power supply various devices without harming our environment. For future research, this design can be extended further for manufacturing and testing of prototypes.

#### REFERENCES

- [1] A. Taybi, A. Tajmouati, J. Zbitou, A. Errkik, M. Latrach, and L. El Abdellaoui, "A new configuration of a high output voltage 2.45 ghz rectifier for wireless power transmission applications," *Telkommika (Telecommunication Computing Electronics and Control)*, vol. 16, no. 5, pp. 1939–1946, 2018, doi: 10.12928/TELKOMNIKA.v16i5.9707.
- [2] S. Ihlou, H. Tizyi, A. Bakkali, A. El Abbassi, and J. Foshi, "Design and development of a microstrip patch antenna array for rectenna system," *ACM International Conference Proceeding Series*. ACM, pp. 323–328, 2020, doi: 10.1145/3419604.3419766.
- [3] T. A. Elwi and A. M. Al-Saegh, "Further realization of a flexible metamaterial-based antenna on indium nickel oxide polymerized palm fiber substrates for RF energy harvesting," *International Journal of Microwave and Wireless Technologies*, vol. 13, no. 1, pp. 67–75, 2021, doi: 10.1017/S1759078720000665.
- [4] T. A. Elwi, D. A. Jassim, and H. H. Mohammed, "Novel miniaturized folded UWB microstrip antenna-based metamaterial for RF energy harvesting," *International Journal of Communication Systems*, vol. 33, no. 6, p. e4305, 2020, doi: 10.1002/dac.4305.
- [5] A. Taybi, A. Tajmouati, J. Zbitou, A. Errkik, M. Latrach, and L. El Abdellaoui, "A new design of high output voltage rectifier for rectenna system at 2.45 GHz," *Indonesian Journal of Electrical Engineering and Computer Science (IJECS)*, vol. 13, no. 1, pp. 226–234, 2019, doi: 10.11591/ijeecs.v13.i1.pp226-234.
- [6] P. C. Kar and M. A. Islam, "Design and performance analysis of a rectenna system for charging a mobile phone from ambient EM waves," *Heliyon*, vol. 9, no. 3, pp. e13964–e13964, Feb. 2023, doi: 10.1016/j.heliyon.2023.e13964.
- [7] M. Kumar, S. Kumar, and A. Sharma, "An analytical framework of multisector rectenna array design for angular misalignment tolerant RF power transfer systems," *IEEE Transactions on Microwave Theory and Techniques*, vol. 71, no. 4, pp. 1835–1847, 2022, doi: 10.1109/TMTT.2022.3222195.
- [8] W. C. Brown, "Experiments involving a microwave beam to power and position a helicopter," *IEEE Transactions on Aerospace and Electronic Systems*, vol. AES-5, no. 5, pp. 692–702, 1969, doi: 10.1109/TAES.1969.309867.
- [9] E. E. Eves, "Beamed microwave power transmission and its application to space," *IEEE Transactions on Microwave Theory and Techniques*, vol. 40, no. 6, pp. 1239–1250, 1992, doi: 10.1109/22.141357.
- [10] W. Brown, "Experiments in the transportation of energy by microwave beam," *IRE International Convention Record*. Institute of Electrical and Electronics Engineers, pp. 8–17, 2005, doi: 10.1109/irecon.1964.1147324.
- [11] W. C. Brown, "The history of power transmission by radio waves," *IEEE Transactions on Microwave Theory and Techniques*, vol. 32, no. 9, pp. 1230–1242, 1984, doi: 10.1109/TMTT.1984.1132833.
- [12] F. Ouberti, A. Tajmouati, N. Chahboun, L. El Abdellaoui, and M. Latrach, "A novel wideband circularly-polarized microstrip antenna array based on DGS for wireless power transmission," *Telkommika (Telecommunication Computing Electronics and Control)*, vol. 20, no. 3, pp. 485–493, 2022, doi: 10.12928/TELKOMNIKA.v20i3.21711.
- [13] W. H. Tu, S. H. Hsu, and K. Chang, "Compact 5.8-GHz rectenna using stepped-impedance dipole antenna," *IEEE Antennas and Wireless Propagation Letters*, vol. 6, pp. 282–284, 2007, doi: 10.1109/LAWP.2007.898555.
- [14] Y. J. Ren, M. Y. Li, and K. Chang, "35 GHz rectifying antenna for wireless power transmission," *Electronics Letters*, vol. 43, no. 11, pp. 602–603, 2007, doi: 10.1049/el:20071061.
- [15] M. A. Sennouni, J. Zbitou, B. Abboud, A. Tribak, H. Bennis, and M. Latrach, "Design and fabrication of a new circularly polarised 2 × 3 antenna array for rectenna system," *International Journal of Engineering Systems Modelling and Simulation*, vol. 9, no. 2, pp. 86–95, 2017, doi: 10.1504/IJESMS.2017.083227.
- [16] S. Almorabeti, H. Terchoune, M. Rifi, H. Tizyi, and S. Smihily, "Smart antenna design alimented by a 4x4 butler matrix," *Telkommika (Telecommunication Computing Electronics and Control)*, vol. 19, no. 4, pp. 1342–1348, 2021, doi: 10.12928/TELKOMNIKA.v19i4.18788.
- [17] J. Zbitou, M. Latrach, and S. Toutain, "Hybrid rectenna and monolithic integrated zero-bias microwave rectifier," *IEEE Transactions on Microwave Theory and Techniques*, vol. 54, no. 1, pp. 147–152, 2006, doi: 10.1109/TMTT.2005.860509.
- [18] W. Huang, B. Zhang, X. Chen, K. Huang, and C. Liu, "Study on an S-band rectenna array for wireless microwave power transmission," *Progress in Electromagnetics Research*, vol. 135, pp. 747–758, 2013, doi: 10.2528/PIER12120314.
- [19] G. A. Vera, A. Georgiadis, A. Collado, and S. Via, "Design of a 2.45 GHz rectenna for electromagnetic (EM) energy scavenging," *2010 IEEE Radio and Wireless Symposium, RWS 2010 - Paper Digest*. IEEE, pp. 61–64, 2010, doi: 10.1109/RWS.2010.5434266.

- [20] E. Falkenstein, M. Roberg, and Z. Popović, "Low-power wireless power delivery," *IEEE Transactions on Microwave Theory and Techniques*, vol. 60, no. 7, pp. 2277–2286, 2012, doi: 10.1109/TMTT.2012.2193594.
- [21] J. Heikkinen and M. Kivikoski, "Low-profile circularly polarized rectifying antenna for wireless power transmission at 5.8 GHz," *IEEE Microwave and Wireless Components Letters*, vol. 14, no. 4, pp. 162–164, 2004, doi: 10.1109/LMWC.2004.827114.
- [22] M. Ali, G. Yang, and R. Dougal, "A new circularly polarized rectenna for wireless power transmission and data communication," *IEEE Antennas and Wireless Propagation Letters*, vol. 4, no. 1, pp. 205–208, 2005, doi: 10.1109/LAWP.2005.851004.
- [23] M. K. Fries and R. Vahldieck, "Uniplanar circularly polarized slot-ring antenna architectures," *Radio Science*, vol. 37, no. 2, p. VIC 5-1-VIC 5-10, 2002, doi: 10.1029/2001rs002569.
- [24] B. Strassner and K. Chang, "5.8-GHz circularly polarized rectifying antenna for wireless microwave power transmission," *IEEE Transactions on Microwave Theory and Techniques*, vol. 50, no. 8, pp. 1870–1876, 2002, doi: 10.1109/TMTT.2002.801312.
- [25] A. A. Lotfi Neyestanak, "Ultra wideband rose leaf microstrip patch antenna," *Progress in Electromagnetics Research*, vol. 86, pp. 155–168, 2008, doi: 10.2528/PIER08090201.
- [26] F. Ouberr, A. Tajmouati, J. Zbitou, I. Zahraoui, and M. Latrach, "A novel design of circularly polarized pentagonal planar antenna for ISM band applications," *Telkomnika (Telecommunication Computing Electronics and Control)*, vol. 19, no. 5, pp. 1484–1489, 2021, doi: 10.12928/TELKOMNIKA.v19i5.19393.
- [27] N. Khu Say Wah and H. M. Tun, "Compact circularly polarized slotted symmetric V slits microstrip patch antenna for ISM band applications," *Asian Journal of Applied Sciences*, vol. 8, no. 6, 2020, doi: 10.24203/ajas.v8i6.6385.
- [28] C. A. Balanis, *Antenna theory: analysis and design*, John Wiley and sons, 3rd Edition, 2016.
- [29] M. A. Sennouni, J. Zbitou, A. Benaissa, A. Tribak, O. Elmrabet, and M. Latrach, "Development of a new slit-slotted shaped microstrip antenna array for rectenna application," *Journal of Emerging Technologies in Web Intelligence*, vol. 6, no. 1, pp. 49–53, 2014, doi: 10.4304/jetwi.6.1.49-53.

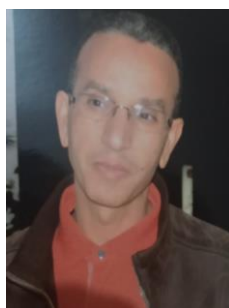
## BIOGRAPHIES OF AUTHORS



**Walid En-Naghma**    received his B.Sc. in physics « electronic option » in 2019 from the Faculty of Sciences of Fez, Dhar El Mahraz University in Morocco. He obtained his M.Sc. in microelectronics, signals and systems from the Faculty of Sciences of Dhar El Mahraz University in Fez-Morocco in 2021. He is currently a Ph.D. student at the computer science, signal, automation, and cognitivism laboratory (LISAC Laboratory) at the Faculty of Sciences of Fez, Dhar El Mahraz University in Morocco. His current research interests include the analysis and conception of microstrip patch antennas and their applications in WPT, MPT and RF energy harvesting as well as the analysis and design of filters. He can be contacted at email: walid.ennaghma@usmba.ac.ma.



**Hanan Halaq**    received the Ph.D. degree in real-time digital holographic interferometry from telecom physique strasbourg (TPS), former École Nationale Supérieure de Physique de Strasbourg (ENSPPS), Illkirch-Graffenstaden, France, in 2010. She is currently an Associate Professor at Faculty of Science Dhar El Mahraz (FSDM) and a researcher at the computer science, signals, automatition and cognitivism laboratory (LISAC), Fez, Morocco. She can be contacted at email: hanan.halaq@usmba.ac.ma.



**Abdelghani El Ougli**    received his Ph.D. degree in Automation, Signals, and Systems from the Faculty of Sciences at Dhar el Mehraz, University of Sidi Mohamed Ben Abdellah in 2009 for his thesis titled "integration of fuzzy techniques in the synthesis of adaptive controllers". He is currently a professor at Sidi Mohamed Ben Abdellah University, a researcher, and a member of the team the computer science, signal, automation, and cognitivism laboratory (LISAC), Faculty of Science, Sidi Mohamed Ben Abdellah University, Fez, Morocco. He can be contacted at email: a.elougli@yahoo.fr.